Control of Autorotational Characteristics of Light-Airplane Fuselages

B. N. Pamadi,* V. Jambunathan,† and A. Rahman†
Indian Institute of Technology, Bombay, India

Single-degree-of-freedom, free-to-roll, autorotational tests in a low-speed wind tunnel are conducted to explore the effects of windward strakes on the autorotational characteristics of typical light-airplane fuselage models. The results indicate that the autorotational speeds are very sensitive to strake height and location. With this technique, it is demonstrated that a large degree of control can be obtained over the autorotational behavior of such light-airplane fuselages.

Nomenclature

b_0 = width of the model
C_y = sectional side-force coefficient, = side force/$(\frac{1}{2}\rho V^2 b_0 \ell)$
h = strake height
ℓ = length of the model
r = distance measured along the bottom surface from vertical side to strake location
R = corner radius
V = freestream velocity
α = angle of attack
$\Delta\omega_0$ = increase/decrease of autorotational speed for strake configuration over the basic model
η = r/b_0
ξ = h/b_0
ρ = density of air
ϕ = two-dimensional crossflow angle
Ω = angular velocity of the model about the wind axis
ω_0 = autorotational speed = $\Omega\ell/2V$

I. Introduction

THE autorotational characteristics of the fuselage have a significant influence on the spin behavior of the light airplane. If the fuselage is prone to autorotation, it attempts to drive the aircraft deeper into spin, i.e., toward a higher angle of attack and spin rate. On the other hand, if the fuselage resists autorotation and is stable, it always tries to restrict the spin to lower angles of attack and spin rates.

Autorotational behavior of a light-airplane fuselage depends on the crossflow aerodynamic characteristics which, in turn, depend on its cross-sectional shape, particularly of its aft portion and Reynolds number.[1-3] The autorotational behavior of light airplanes can be altered by effecting minor modifications to the airframe. One such example is the installation of strakes on the underside of the fuselage. In Ref. 4, the strakes mounted on the bottom of the fuselage were found to alter the spin behavior of the model of a light general-aviation airplane. On the model, the strakes were found to be effective in slowing down the spin rate and also in eliminating the flat spin mode of the basic model. However, the same strakes tested on the corresponding full-scale airplane[5] were not effective in preventing the development of the flat spin mode. The flight test aircraft, however, differed from the spin-tunnel model in that the former had the full-span drooped-wing leading edge, which was recognized to have a strong prospin tendency.

In Ref. 6, the effect of strakes on the autorotational characteristics of a sharp-cornered, noncircular cylinder at low speeds and low Reynolds number was systematically investigated through single-degree-of-freedom, free-to-roll autorotational tests and pressure measurements on the corresponding two-dimensional cylinder in crossflow. The results of this study indicated that the autorotational speeds are very sensitive to strake height and their location on the underside. Depending on their location, strakes can either enhance or reduce the autorotational speed. A result of particular interest is that there is an optimum strake location for which reductions of the order of 75% in autorotational speeds were indicated.

In this paper, the concept of Ref. 6 is developed further for application to light-airplane fuselages. We have considered the fuselage in isolation so that the results of this study can form the basis for later studies considering the mutual interference effects relating to wing and tail surfaces. Also, such an approach helps us to have a better understanding of the aerodynamics of basic fuselage and strake configurations in autorotation/spin. It is quite possible, however, that the interference effects not included here may be significant and may have an influence on the nature of predictions made.

The purpose of this investigation is twofold:

1) To explore the possibility of reducing autorotational speeds for the configurations that are highly autorotative. Light-airplane fuselages whose aft cross sections have sharp-bottom corners like the noncircular cylinder of Ref. 6 belong to this category.

2) To enhance the autorotational tendency of the configurations that are less prone to autorotation. Fuselages having well-rounded bottom surfaces belong to this class.[3]

The results of this experimental study on typical light-airplane fuselage models of the two types just described indicate that a large degree of control can be obtained over the autorotational/spin behavior of isolated fuselage models.

II. Experimental Work

The autorotational, single-degree-of-freedom, free-to-roll tests were carried out in an open jet low-speed wind-tunnel test facility. The nozzle exit cross section of this tunnel is elliptical, with major and minor axes measuring, respectively, 76 cm (30 in.) and 35 cm (13 in.). The maximum air speed of this facility is 35 m/s (115 ft/s). A schematic arrangement of the setup is presented in Fig. 1.

The test models were mounted on a shaft that is housed in a ball-bearing assembly and is free to roll about the wind axis. The model is attached to the shaft through s-shaped linkage designed to give a specified angle of attack (α) to the test model. Four such linkages were fabricated for angles of attack of 25,

Received Dec. 4, 1986; presented as Paper 87-0349 at the AIAA 25th Aerospace Sciences Meeting, Reno, NV, Jan. 12–15, 1987; revision received Nov. 13, 1987.

*Professor, Department of Aeronautical Engineering; currently Senior Research Scientist, Vigyan Research Associates Inc., Hampton, VA. Member AIAA.

†Undergraduate Student, Department of Aeronautical Engineering.

45, 60, and 90 deg. The models are so mounted that their centers of gravity fall on the axis of rotation and are, as such, statically balanced.

The geometry of the test models and strake configurations is presented in Figs. 2–5. The fuselage model A (Fig. 2) is an approximately 1:21 scaled version of the fuselage of the full-scale aircraft of Refs. 4 and 5. For this airplane, both the spin-tunnel model[4] and full-scale flight test aircraft[5] exhibited the developed flat spin modes. Thus, this model (A) belongs to the type 1 category mentioned earlier. The purpose of the investigation for this model is therefore to explore the possibility of reducing the autorotation/prospin tendency. The noncircular cylindrical model tested in Ref. 5 had the same cross-sectional shape as the aft section of this airplane fuselage.

Model B (Fig. 3) is an approximately 1:22 scaled version of the light airplane of Ref. 7. The aft fuselage sections of this airplane have well-rounded corners with corner radii R ranging from 15 to 20%. This airplane exhibits a steep spin mode only and does not enter a developed flat spin mode. Thus, this model (B) can be considered to belong to the second category. For fuselage model B, two test models were made: 1) the fuselage model (1:22 scale) and 2) the simple noncircular cylindrical model fitted with a well-rounded nose, with the cross section of the cylindrical part representative of the aft geometry of this airplane fuselage. The well-rounded nose is fitted to produce smooth flow over the model.

The autorotational tests on cylindrical models having a constant cross section like that of the aft fuselage help us to examine to what extent the test results on these idealized models are representative of the corresponding fuselage models. If we could establish a good measure of confidence in this correlation, it can be usefully employed to save time and effort involved in such testing.

For fuselage models A and B, part-length strakes for the straight portion aft of center of gravity were installed as shown in Fig. 4. For cylindrical model B, full-length strakes were employed (Fig. 5). Strake heights of $\xi = 0.1$, 0.2, and 0.3 were tested on fuselage model A with strake locations at $\eta = 0$, 0.2, and 0.5. More strake locations were difficult on account of small model size. For the cylindrical model B, strake heights ranged from 0.1 to 0.5, and location was systematically varied from $\eta = 0.1$ to 0.5. The strake could not be adequately fixed between $\eta = 0$ and 0.1 on account of corner radius. Three strake heights were used for tests on fuselage model B ($\xi = 0.1$, 0.3, and 0.5), with locations at $\eta = 0.1$, 0.3, and 0.5; once again, limitations arose because of small model size, particularly in the aft region.

The models were fabricated out of balsa wood and were given a smooth-surface finish. The strakes were cut out of thin plastic sheet and attached to the model with adhesive tape.

To begin with (wind off), the test model was positioned in the uniform-velocity zone of the jet and held stationary at a given angle of attack. The wind tunnel was then started and the model given a slight prerotation. If the model is prone to autorotation, it quickly accelerates and attains a stable autorotational speed. On the other hand, if the model is not of autorotational type, the imparted disturbance quickly dies out,

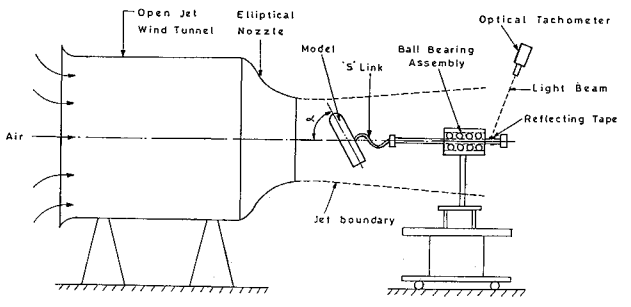

Fig. 1 Schematic diagram of experimental setup.

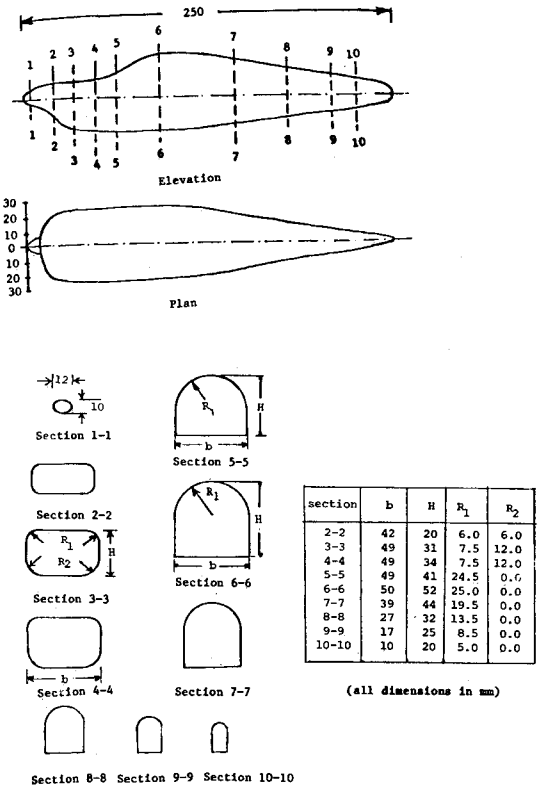

section	b	H	R_1	R_2
2-2	42	20	6.0	6.0
3-3	49	31	7.5	12.0
4-4	49	34	7.5	12.0
5-5	49	41	24.5	0.0
6-6	50	52	25.0	0.0
7-7	39	44	19.5	0.0
8-8	27	32	13.5	0.0
9-9	17	25	8.5	0.0
10-10	10	20	5.0	0.0

Fig. 2 Fuselage of model A.

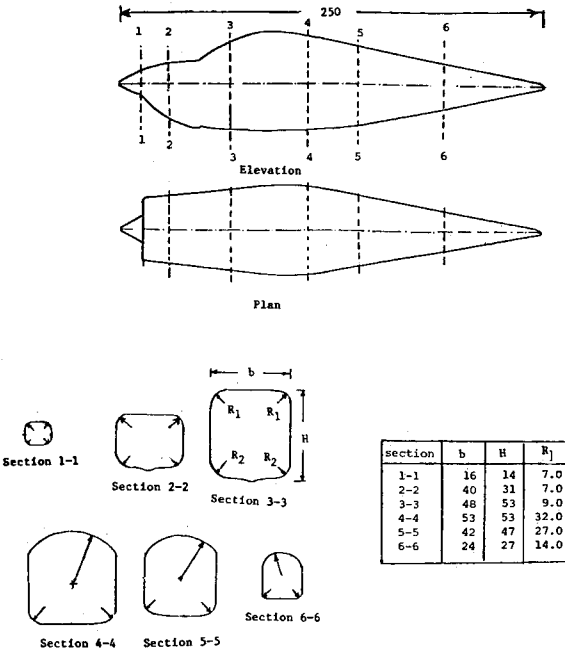

section	b	H	R_1	R_2
1-1	16	14	7.0	4.0
2-2	40	31	7.0	8.0
3-3	48	53	9.0	11.0
4-4	53	53	32.0	10.0
5-5	42	47	27.0	6.0
6-6	24	27	14.0	5.0

Fig. 3 Fuselage of model B.

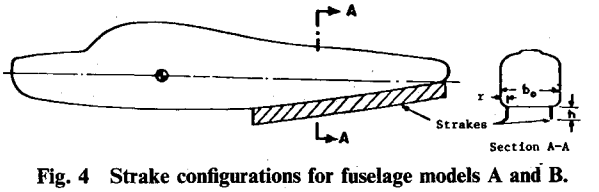

Fig. 4 Strake configurations for fuselage models A and B.

and the model returns to its initial stationary position. Autorotational speeds were measured by a digital noncontact-type optical tachometer.

The test Reynolds number based on the model length was around 3×10^5.

III. Results and Discussion

The measured autorotational speeds of various test models are presented in Figs. 6 to 12, where some typical results of Ref. 6 on cylindrical model A are included in Figs. 6 and 8.

Model A

Basic Models

The autorotational speeds of both noncircular cylinder and fuselage models increase with α (Fig. 6). At lower angles of attack, the fuselage model exhibits relatively higher autorotational speeds compared to the cylindrical model. This difference apparently relates to the hemispherical nose, whose side force and moments about the axis of rotation have a damping effect. At low angles of attack, the autorotative moments produced by the cylindrical sections are small in magnitude (but exceed the magnitude of damping moment) because of lower crossflow dynamic pressure ($\frac{1}{2}\rho V^2 \sin\alpha$). As a result, the cylindrical model has a lower autorotational speed. At higher angles of attack, the autorotative moments generated by the cylindrical sections increased in magnitude because of higher crossflow dynamic pressure. This leads to sharp increase of autorotational speeds for the cylindrical model. For the fuselage model, however, the autorotational speed at higher angles of attack shows a steady rise and a tendency to level off. This pattern can be attributed to the gradual reduction in the area of aft cross sections due to geometrical tapering. As we know, the aft sections are chief contributors to autorotative moment because of their large moment arm.

Strake Configurations

As discussed in Ref. 5, for cylindrical model A, no change in autorotational speeds (compared to the basic model) were found to occur when the strakes were located at, or close to, the corners. When the strakes were moved inward, however, drastic reductions were found to occur, with minimum values noted at $\eta = 0.2$. Further movement of strakes toward the center resulted in an increase in ω_0. At $\eta = 0.50$, the values of ω_0 were close to that of the basic model. The results on the fuselage model (Fig. 7) follow the identical trend, and strake configuration $\xi = 0.3$, $\eta = 0.2$ gives optimum benefit.

The minimum values of autorotational speeds that occur at $\eta = 0.2$ are plotted in Fig. 8. The magnitudes of reduction for the optimum strake configuration ($\xi = 0.3$, $\eta = 0.2$) are of the order of 75–80% for the cylindrical model, which has full-length strakes. Nearly the same values are obtained for the fuselage model (except at $\alpha = 25$ deg) with only partial-length aft strakes.

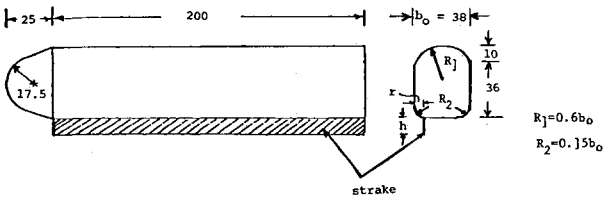

Fig. 5 Cylindrical model B (all dimensions in mm).

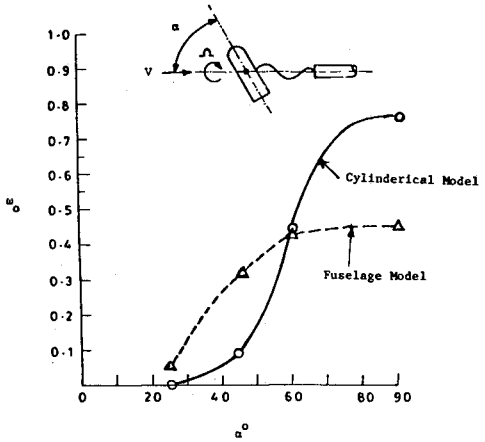

Fig. 6 Autorotational speeds of basic models A.

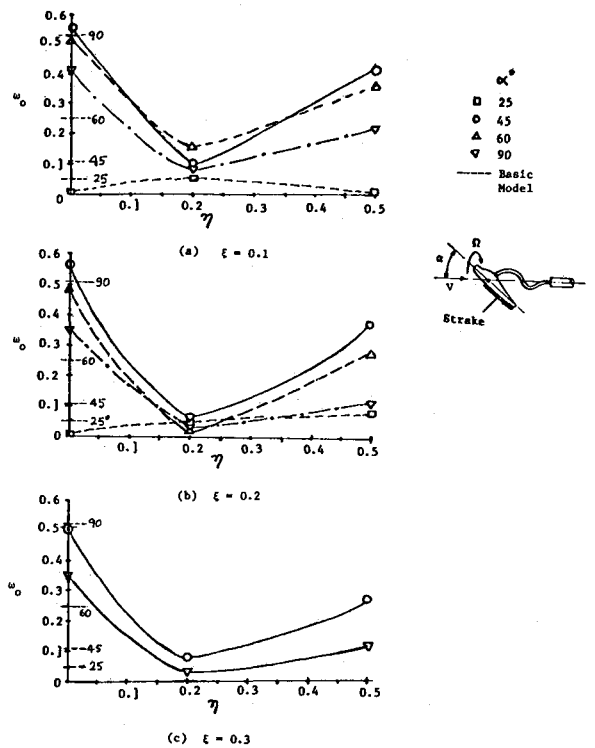

Fig. 7 Effects of strakes on fuselage model A.

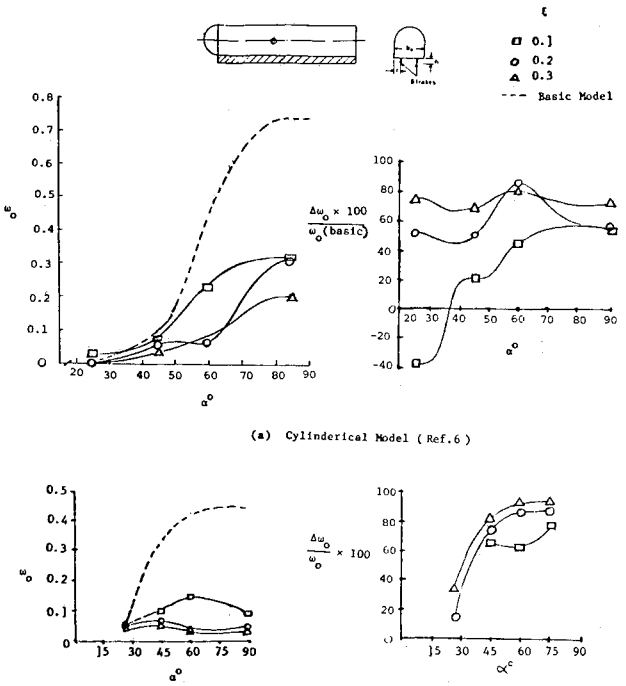

Fig. 8 Variation of minimum ω_0 with α and ξ for models A.

These results indicate that the present technique is potentially capable of slowing down the autorotational speeds/spin behavior of light general-aviation airplanes exhibiting flat spin mode.

Model B

Basic Models

The variation of autorotational speed of cylindrical and fuselage models with angle of attack is given in Fig. 9. The fuselage model displays much higher values of ω_0 compared to the cylindrical model. The reason for this difference appears to be the presence of a well-rounded nose on the cylindrical model, which generates damping moments, as mentioned earlier. Since the autorotative moments of aft cylindrical sections are smaller due to corner rounding, the autorotational speeds of the cylindrical model remain small, compared to those of fuselage model, at all angles of attack.

Strake Configurations

The effect of strakes employed in pairs was similar to that found on model A and resulted in drastic reductions in ω_0. These results are not presented here because the purpose of the investigation of this model was to explore the possibility of enhancing the autorotational speed. A single strake installed on the bottom surface was found to serve this purpose, and these test results are presented in Fig. 10. Generally, for $0.1 < \eta < 0.4$, the autorotational speeds for all strake heights, $\xi = 0.1$–0.5, were much higher compared to the basic model except at $\alpha = 90$ deg, where a minimum around $\eta = 0.2$–0.3 and a second maximum close to $\eta = 0.4$ were recorded for strake heights of $\xi = 0.1$–0.30. However, when the strake height was higher, e.g., $\xi = 0.4$ and 0.5, this behavior at $\alpha = 90$ deg vanished, and a consistent trend of variation of ω_0 with η was obtained. The maximum values of ω_0 were obtained when the single strake was located at $\eta = 0.1$. Placing the strakes inward of this point results in lower values of ω_0. Therefore, this strake location of $\eta = 0.1$ is regarded as optimum for enhancing the autorotation/spin behavior of this model, which belongs to the second category of light-airplane fuselages. The results for fuselage model B (Fig. 11), with single aft strake, follow the same trend as that of the cylindrical model. However, for $\alpha > 60$ deg, the autorotational speeds of fuselage models with strakes at $\eta = 0.10$ fall below the value of the basic model, as shown in Fig. 12b.

The maximum values of ω_0 occurring at $\eta = 0.1$ are presented in Fig. 12. It is interesting to note that large increases in ω_0, ranging up to 1800%, are obtained for the cylindrical model. The fuselage model, with partial-aft-length strakes, displays relatively smaller increases, but these incrementals are still substantial (up to 250%) compared to the basic fuselage model.

The close agreement between the test results on cylindrical and fuselage models indicates that employing a cylindrical model having a cross section representative of aft fuselage geometry gives satisfactory predictions of autorotational characteristics of light-airplane fuselages. Therefore, this simplified approach, that is, testing idealized cylindrical models, can be usefully employed in autorotational/spin studies to save considerable testing time and effort.

Flow Mechanism

The crossflow aerodynamic characteristics of the body play a major role in determining its autorotational behavior. These characteristics depend on cross-sectional geometry and Reynolds number. Of particular importance is the variation of side force with crossflow angle of aft sections because of their large moment arms.

On a rotating model (Fig. 13), the crossflow angle is given by

$$\phi = \tan^{-1}(\Omega x/V)$$

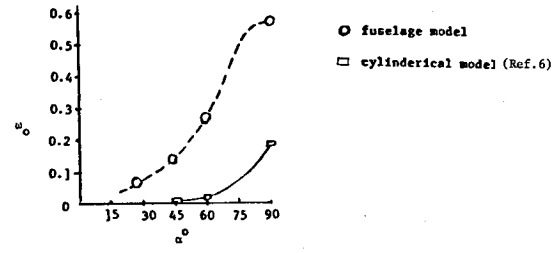

Fig. 9 Autorotational speeds of basic models B.

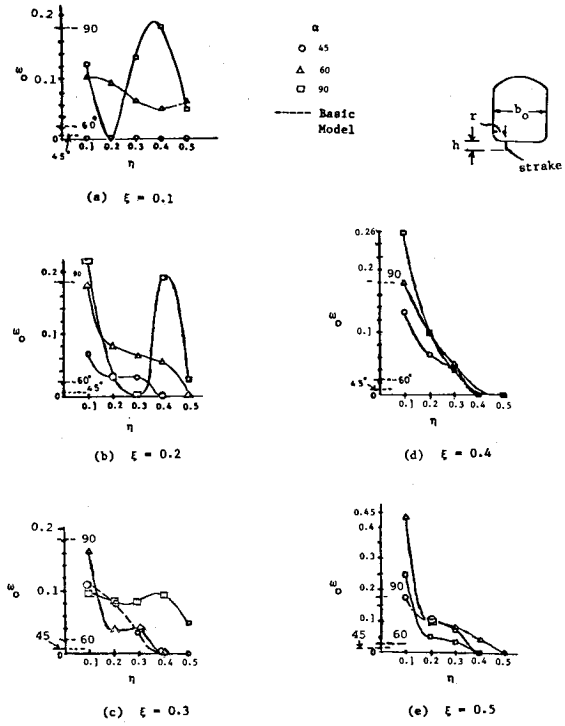

Fig. 10 Effect of single strake on autorotational speeds of cylindrical model A.

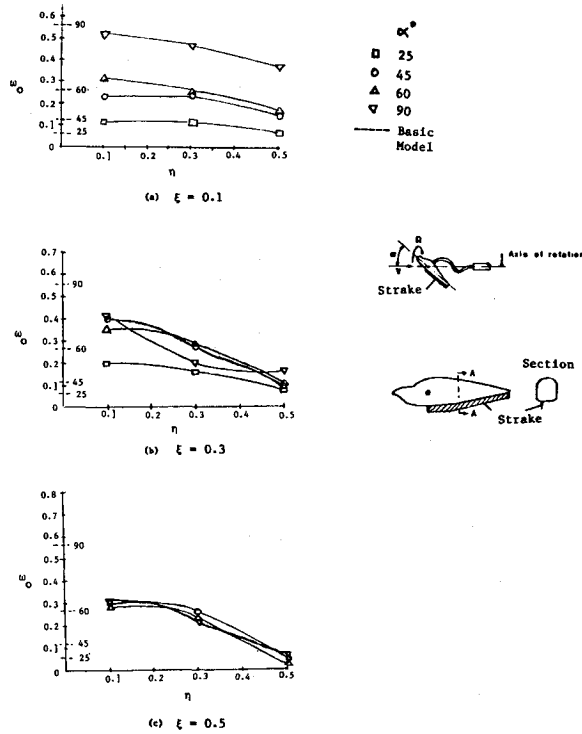

Fig. 11 Effects of single strake on autorotational speeds of fuselage model B.

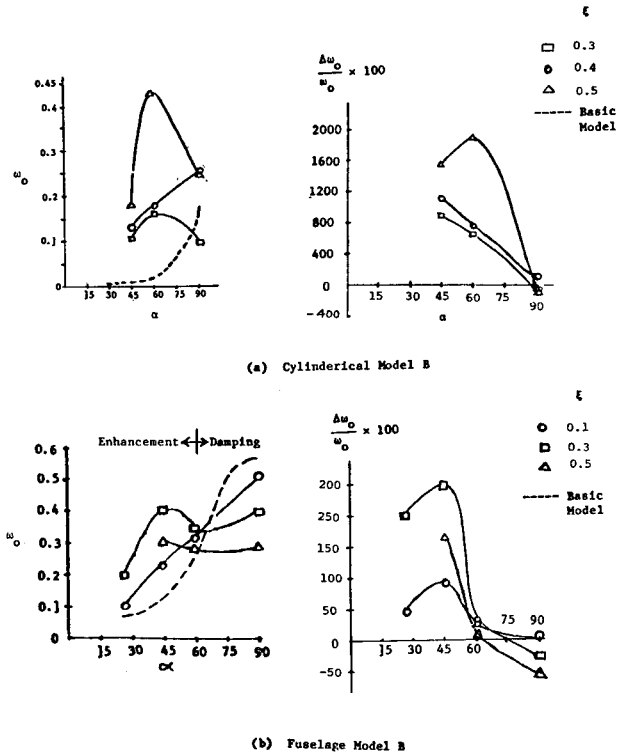

Fig. 12 Maximum autorotational speeds at $\eta = 0.1$.

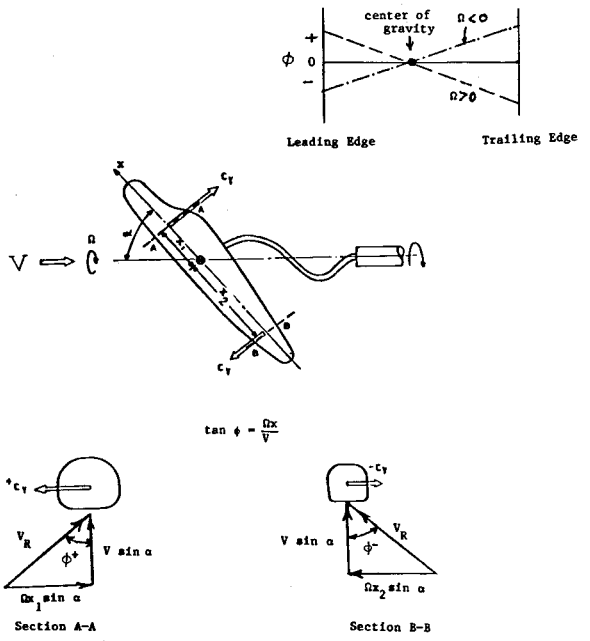

Fig. 13 Schematic sketch of a rotating model.

For autorotation, Ω is constant, and the net moment about the axis of rotation passing through the center of gravity is zero.

The variation of sectional side force can be broadly classified into two types (Fig. 14). The side-force variation of type I, where the side-force coefficient is positive for some values of ϕ (and vice versa for negative values of ϕ), gives rise to instability and autorotation. A model having side-force variation of type II is stable. The flow patterns[3] associated with these basic types are also shown in Fig. 14.

The installation of strakes alters the pressure field and side-force characteristics of the cross section of the model. Depending on their location, the strakes produce significant side forces, which can either enhance or dampen the autorotational

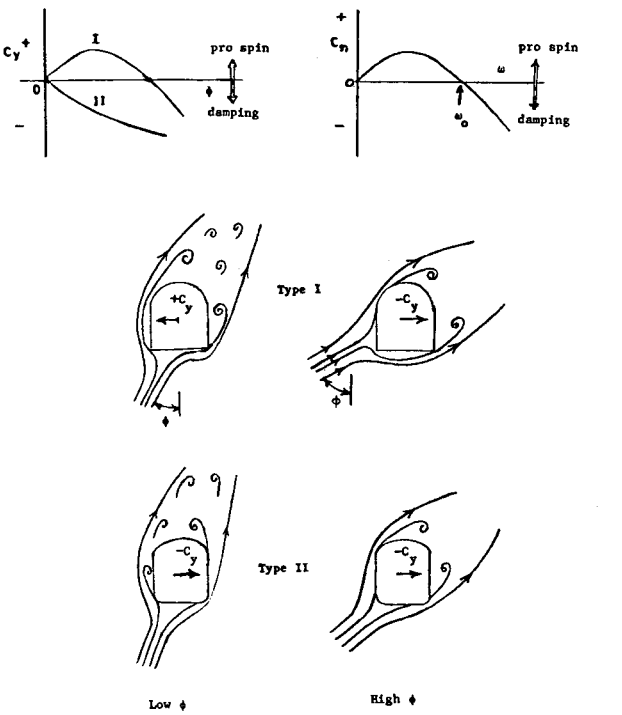

Fig. 14 Typical crossflow aerodynamic characteristics of noncircular cylinders.

tendency of the model. In Ref. 6, detailed two-dimensional (crossflow) pressure tests over the noncircular section of model A were carried out with several strake configurations. Similar two-dimensional pressure distribution tests for model B were carried out in Ref. 8. Based on this pressure distribution data base, it has been possible to identify certain distinct flow patterns for each model, as sketched in Figs. 15 and 16.

Model A

For model A, three types of flow patterns occur, depending on the strake location. When the strakes are at, or very close to, the corners, the flow turns sharply at each strake, producing positive and negative pressures on the strake surfaces as shown in the type I pattern (Fig. 15). The separated flow on the windward strake reattaches to the model surface where, as on the leeside strake, it remains separated. The side forces acting on each strake are nearly equal to each other and cancel. Thus, there is not much change in the autorotational tendency, as noted for strakes at $\eta = 0$ (see Fig. 7).

When the strakes are located around $\eta = 0.2$, the type II flow pattern was found to occur. The flow appears to be avoiding the sharp turn at the windward strake while still turning sharply on the leeside strake. This results in a much higher value of side force on the leeside strake (C_{ys2}) compared to the windward strake (C_{ys1}). This produces a damping effect, which results in a drastic fall in ω_0, as observed for $\eta = 0.2$ (Fig. 7).

With further movement of strakes toward the center, type III flow pattern occurs, which produces a damping side force on the strake assembly, but magnitudes are lower. With a single strake at the center ($\eta = 0.5$), much of the damping effect produced by strake assembly is lost, and ω_0 comes close to that of the basic model.

Model B

With a single strake at, or close to, $\eta = 0.1$, the flow pattern of type I occurs (Fig. 16). Here the flow turns sharply over the strake, producing large pressure differentials across the strake and a side force on the strake that will enhance autorotational tendency. For any other strake location, $0.1 < \eta < 0.5$, the flow pattern of type II occurs where the strake produces a damping

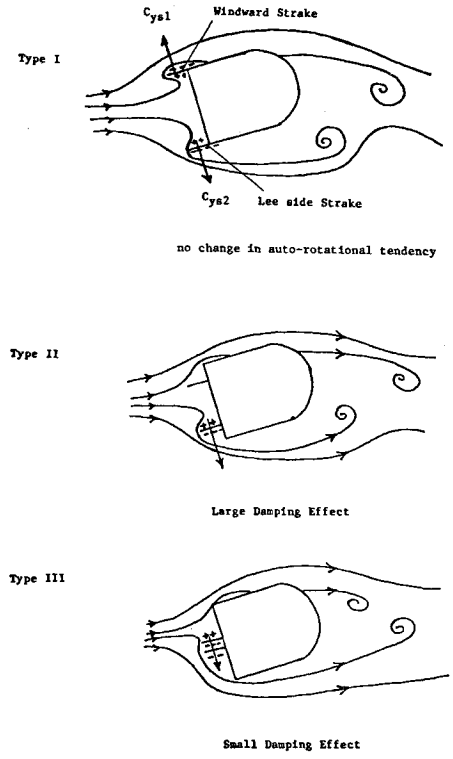

Fig. 15 Types of flow patterns associated with various strake locations for model A.

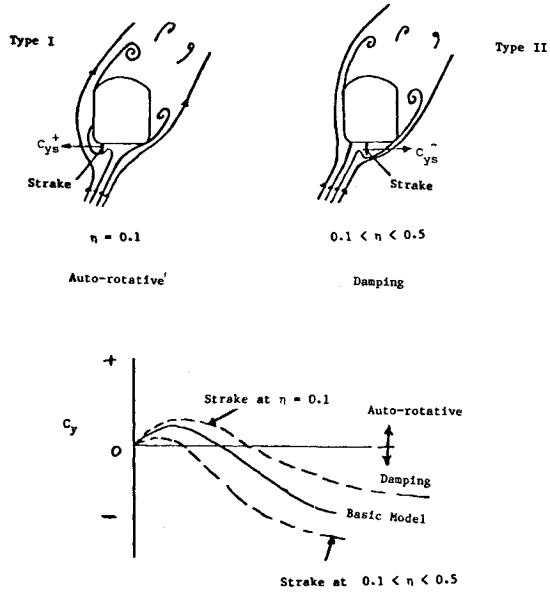

Fig. 16 Types of flow patterns associated with various strake locations for model B.

effect, leading to a drop in ω_0, which becomes increasingly prominent as the strake is moved toward the center.

Effect of Reynolds Number

The effect of Reynolds number has not been directly addressed in this study. Since the flow pattern and side forces acting on the strakes are determined mainly by the flow directions and pressure fields around the strakes, which are fixed by strake height and locations, the Reynolds number should not have much effect. However, the transition in the separated flow leaving the strakes and subsequent reattachment back to the model surface can have a dependence on the Reynolds number. Further investigation is necessary to have a clear understanding of this problem.

Comparison with Spin-Tunnel and Flight Test Results

The installation of strakes produced beneficial effects in the spin-tunnel model tests conducted on the model A airplane.[4] Certain strake configurations were found to be effective in slowing down the spin rate and eliminating the flat spin mode of the model. The corresponding modifications made to the flight test model A airplane were not effective, however, and the airplane continued to exhibit the flat spin mode. These contradictory test results raise a doubt about the usefulness of installing strakes on the underside of the fuselage to control the spin behavior of light general-aviation airplanes. This question will now be addressed and an explanation presented to solve the apparent discrepancy.

The flight test aircraft was fitted with a full-span drooped leading edge on both wings. The spin-tunnel model had conventional wings. Thus, there is a fundamental difference in the configurations tested in the spin-tunnel and flight tests.

The model A airplane has the spin modes for the aileron neutral case (tail 4) specified in Table 1. Notice that the presence of the drooped leading edge on the wing leads to significantly higher angles of attack and spin rates. The drooped leading edge is, therefore, a strong driving force in spin, as recognized in Ref. 5.

Let us consider the airframe modifications tried in spin-tunnel and full-scale flight tests (Fig. 17) and discuss these results against the background of the present work.

Vertical Fins on Fuselage Bottom

This modification proved very effective on the spin-tunnel model in that the flat spin mode was eliminated and the model entered the steep spin mode slowly. On the full-scale airplane with drooped leading edge, however, this modification did not prove effective because the driving or prospin effect of the drooped leading edge overrode the damping effect produced by the vertical fins/strakes.

In spin-tunnel tests, in addition to the value of $r/b_0 = 0.067$ (Fig. 16a), other values of $r/b_0 = 0.0$, 0.104, and 0.208 were tried. The corner strake ($r = 0$) was found to be ineffective, and the strakes located slightly inward ($r/b_0 = 0.066$ and 0.104) were found to be effective. However, as the strakes were moved farther inward, say, $r/b_0 = 0.208$, the beneficial effect was lost, and the model entered the flat spin mode. These results are very similar to the present results. Further, the present work identifies optimum strake configurations and quantifies the beneficial effect produced by the installation of strakes in terms of reduction in autorotational speeds. The spin-tunnel test results, however, are qualitative.

Semicircular Cylinders

The corner radius ($R/b_0 = 0.066$) did not produce any beneficial effect in either the model or full-scale flight tests. This is not surprising because Polhamus' data[3] show that a cylinder with 8% corner radius had the pro-spin side-force variation of type I, discussed earlier. Further, Polhamus' data[3] show that, for this type of modification to be effective, corner radius should be much higher, say, 20% or more.

Table 1 Spin modes for aileron neutral case (Model A, Tail 4)

	Spin-tunnel model tests[4]	Full-scale flight tests[5]
Steep spin		
Angle of attack, deg	38	51
Ω deg/s	144	157
Flat spin		
Angle of attack, deg	68	77
Ω deg/s	209	324

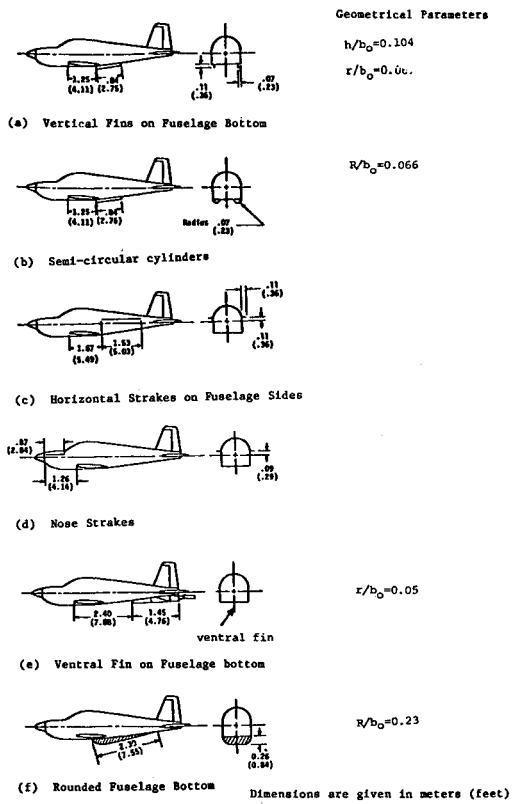

Fig. 17 Minor modifications tested in full-scale and spin-tunnel tests.[4,5]

Horizontal Strake on Fuselage

This case was marginally effective on the spin-tunnel model. The spin-tunnel model still entered the flat spin mode. Obviously, on the full-scale aircraft, this modification could not be effective on account of the drooped leading edge.

Nose Strake

This modification was not tried on the spin-tunnel model. Also, this case was not found effective on the full-scale airplane because of the drooped leading edge.

Ventral Fin

Spin-tunnel tests were conducted to evaluate the effectiveness of this modification under the so-called criterion spin.[4] On the model, this modification was effective in eliminating the flat spin, and the steep spin mode was rendered steeper. On a full-scale airplane, the modification was not effective. The ventral fin is similar to the present case of central strake.

Rounded Fuselage Bottom

Here the corner rounding is about $R/b_0 = 0.23$. The modification is effective in preventing the flat spin mode of the model because, as said earlier in this section, the rounding of the corners beyond 20% produces the side-force variation of type II shown in Fig. 14. On a full-scale airplane with drooped leading edge, however, the damping effect resulting from corner rounding may not be sufficient to compensate for the driving force of the drooped leading edge.

IV. Concluding Remarks

An experimental investigation at low (model) Reynolds numbers is conducted to evaluate the effect of strakes on typical light-airplane fuselage models. The results of this study indicate the possibility of establishing a large degree of control over autorotational behavior of light-airplane fuselages with installation of strakes. For airplanes with aft fuselage geometries similar to model A, the strakes can be employed to soften the prospin behavior of the fuselage and thereby reduce the possibility of flat spin. For fuselages of type B having rounded bottoms, a single strake can be employed to generate autorotative or prospin moments to drive the airplane deeper into spin if required, e.g., on a trainer aircraft. Thus, the present results indicate the possible autorotational tailoring of light-airplane fuselages by appropriate installation of strakes. The strakes can be retracted into the fuselage when their presence in the airflow is not desired.

In spin-tunnel model tests,[4] the technique of installing the strakes on the bottom side of the fuselage for generating spin damping effect proved successful for light general airplanes with conventional wing sections. However, for the full-scale aircraft fitted with a full-span drooped leading edge, these devices were found to be ineffective in eliminating the flat spin mode.[5]

The strake lengths and heights tested in the present study are much greater than those employed in spin-tunnel and full-scale flight tests. Further, it has been found that, for fuselage model A, strakes themselves produce significant side force and damping effects when at optimum location. The optimum strake configurations identified in this study could be capable of providing adequate damping effect to prevent a conventional-wing light airplane from entering a flat spin. Further work is necessary, however, to ascertain the suitability of the strakes to counter the strong prospin effect generated by such devices as the full-span drooped leading edge.

References

[1]Clarkson, M. H., "Auto-Rotation of the Fuselage," Design Aerodynamic Session, IAS 26th Annual Meeting, New York, Jan. 27–30, 1958, IAS Reprint No. 770.

[2]Beaurain, L., "General Study of Light Airplane Spin, Aft Fuselage Geometry, Part I," NASA TTF-17446, 1977.

[3]Polhamus, E. C., "Effects of Flow Incidence and Reynolds Number on Low Speed Aerodynamic Characteristics of Several Non-Circular Cylinders with Application to Directional Stability and Spinning," NASA TR R-29, 1959.

[4]Burk, S. M., Bowman, J. S., and White, W. L., "Spin Tunnel Investigations of the Spinning Characteristics of Typical Single Engine General Aviation Airplane Designs, Part I, Low-Wing Model A: Effect of Tail Modification," NASA TP-1009, Sept. 1977.

[5]Stough, H. P., III and Patton, J. M., Jr., "The Effect of Configuration Changes on Spin and Recovery Characteristics of a Low-Wing Research Airplane," AIAA Paper 79-1786, 1979.

[6]Pamadi, B. N. and Pordal, H. S., "Effect of Strakes on the Auto-Rotational Characteristics of Non-Circular Cylinders," *Journal of Aircraft*, Vol. 24, Feb. 1987, pp. 84–97.

[7]Bihrle, W., Jr. and Hultberg, R. S., "Rotary Balance Test Data for a Typical Single Engine Aviation Design for AOA Range 8° to 90°, Part I—High Wing Model B," NASA CR-3097, Sept. 1979.

[8]Pereira, C., "Effect of Strakes on the Cross-Flow Characteristics of Noncircular Cylinders," undergraduate, Project Report, Department of Aeronautical Engineering, Indian Institute of Technology, Bombay, India, 1986.